Magnetic Field Effects on the Photochemical Electron-Transfer Reactions of 10-Methylphenothiazine and Dicyanobenzene Derivatives in Nonviscous Homogeneous Solutions

Yoshio Sakaguchi[†] and Hisaharu Hayashi*

Molecular Photochemistry Laboratory, The Institute of Physical and Chemical Research (RIKEN), Wako, Saitama 351-01, Japan

Received: June 27, 1996; In Final Form: October 14, 1996[⊗]

Magnetic field effects on the photochemical electron-transfer reactions of 10-methylphenothiazine with 1,4-dicyanobenzene and tetrafluoro-1,4-dicyanobenzene are investigated by a nanosecond laser photolysis technique. For these reactions, the recombination of the geminate radical ion pairs as well as the yields and decay rates of the escaped radical ions showed clear magnetic field dependence in nonviscous homogeneous solutions. The mechanisms of the magnetic field effects are ascribed to the hyperfine coupling and Δg mechanisms at low and high magnetic fields, respectively. The smaller magnetic field effects on the reaction of the fluorinated derivative than those of 1,4-dicyanobenzene are ascribed to its smaller back-electron-transfer rate because its free-energy change is smaller than that of the nonsubstituted one.

1. Introduction

Twenty years ago, magnetic field effects (MFEs) on photochemical and photophysical processes of excited molecules were still covered with a veil of secrecy. During the last 2 decades, however, MFEs on such processes have been studied extensively not only in condensed phases but also in the gas phase,[1−3] and the progress in these studies has brought about the advent of a new research field encompassing chemistry, physics, and biology. Prof. Saburo Nagakura named this new field "(dynamic) spin chemistry", together with related phenomena such as chemically induced dynamic nuclear and electron polarization (CIDNP and CIDEP). He and his group have been leaders in the establishment of spin chemistry.

In 1966, Nagakura's group first made a general study on the singlet−triplet (S−T) mixing of radical pairs (RPs), taking a RP trapped in a single crystal as an example.[4] This RP mechanism has become one of the fundamentally important theories in explaining not only MFEs and magnetic isotope effects (MIEs) on chemical reactions in solution but also CIDNP and CIDEP.[1−3] His group also found MFEs on the yields of cage and escape products in a singlet-sensitized reaction of dibenzoyl peroxide in toluene at room temperature in a range of magnetic fields (B's) between 0 and 6 T using superconducting magnets,[5−7] explaining these MFEs by the enhancement in the S−T conversion of a generated singlet RP due to the difference of isotropic g factors (the Δg mechanism).[6] This is one of the earliest works about MFEs on photochemical reactions in solution.

Since 1980, we have been studying MFEs on the dynamic behavior of RPs in solution,[8] using nanosecond laser photolysis techniques. In the course of these studies, we have found many new MFEs and MIEs.[1−3] For example, we have found large MFEs and MIEs on RP lifetimes and escape radical yields of many reactions from triplet precursors in micellar solutions at $B < 1.34$ T[1−3,8,9] and succeeded in explaining these MFEs and MIEs in terms of the spin relaxation of triplet RPs (the relaxation mechanism).[9,10] We also found an alternating emissive/absorptive (E/A) phase pattern in each hyperfine line of the CIDEP spectra observed for some RPs in micellar solutions.[11] Later, McLauchlan's[12] and Closs's[13] groups independently explained such peculiar phases in terms of spin-correlated RPs.

Using a superconducting magnet and a double-beam detection system, we have recently developed a nanosecond laser photolysis apparatus with high accuracy and started to measure RP dynamics up to $B = 10$ T.[14,15] Under such large fields, we have found many MFEs on reactions of light-atom-centered radicals like C and O radicals as well as those of heavy-atom-centered ones such as Si, P, S, Ge, and Sn radicals in micellar solutions.[16] These MFEs have been explained by the relaxation and Δg mechanisms.[16]

The MFEs of the radical ion pairs (RIPs) in homogeneous solutions have been investigated intensively since the earliest stage of the studies of MFEs, but these experiments have almost been limited to low magnetic fields of less than 0.4 T.[1,17] Here, the observed MFEs were mainly interpreted in terms of the hyperfine coupling mechanism. Furthermore, the studies of triplet RIPs have been much rarer than those of singlet RIPs.[1] In the present study, we investigated typical electron-transfer reactions from the triplet excited state of 10-methylphenothiazine (^{3}MPTZ*) which includes a heavy atom, sulfur. The RIPs from ^{3}MPTZ* and electron acceptors have large g differences between the component radical ions. By applying high magnetic field, we could observe MFEs due to the Δg mechanism (ΔgM) which are rare in the studies of RIPs in homogeneous solutions.

2. Experimental Section

10-Methylphenothiazine (MPTZ, Kanto Chemical Co.) and 1,4-dicyanobenzene (DCNB, TCI) were recrystallized from ethanol and from an ethanol−benzene mixture, respectively. Tetrafluoro-1,4-dicyanobenzene (F_4DCNB, Aldrich) was used without further purification. 2-Propanol (2-PrOH), benzene of Cica−Merck high-performance liquid-chromatography grade, and dimethyl sulfoxide (DMSO) of Cica−Merck UV analysis grade were used as solvents without further purification. The detergent, Brij35 (TCI), was used without further purification.

* E-mail: ysakaguc@postman.riken.go.jp. Fax: ++48-462-4664.
[†] E-mail: hhayashi@postman.riken.go.jp.
[⊗] Abstract published in *Advance ACS Abstracts,* December 15, 1996.

S1089-5639(96)01907-X CCC: $14.00

Water (>18 MΩ cm) was obtained from an Iwatani UP-100 ultrapure water maker.

Laser flash photolysis experiments were performed at 293 K. The magnetic fields of $B = 0-1.75$ T were generated by a Tokin SEE-10W electromagnet. Those of $B = 0-10$ T were generated by an Oxford 37057 superconducting magnet with a PS120-10 power supply. Solvents were degassed by sonication, and the solutions were prepared under nitrogen atmosphere. The sample solution flowed in a 5-mm optical length quartz cell in the sample holder. The sample solutions except for the detergent one were bubbled with pure nitrogen gas during the measurements. The reservoir bottle of the detergent solution was kept under nitrogen during the experiments. The sample solutions were excited with the third (355-nm) harmonic of a Quanta-Ray GCR-103 Nd:YAG laser. For high accuracy measurements, both of the monitoring lights before and after the sample cell were measured. The outputs of the photomultipliers (Hamamatsu R636) were measured by a HP54510A (1 Gs/s) or a HP54522A (2 Gs/s) digitizing oscilloscope and then recorded with a NEC PC9801 computer. Other conditions are similar to those described elsewhere.[14,18] The experiments under the lowest magnetic field ($B < 0.2$ mT for the electromagnet, $B < 0.3$ mT for the superconducting magnet) are denoted as those in the absence of a magnetic field.

A JEOL RE-1X X-band spectrometer was used for the time-resolved ESR measurements without field modulation at room temperature with a XeCl laser (308 nm) of a Lumonics EX-742 excimer laser as an exciting light source. The output signal was averaged by an SRS SR250 boxcar integrator. Other experimental conditions are similar to those described elsewhere.[19]

3. Results and Discussion

In the present study, we would like elucidate the dynamic behavior of the RIPs at large magnetic fields. Here, the present reaction systems and their MFEs are investigated for the first time. In order to discuss the MFEs due to the ΔgM at large fields, we must discuss the reaction mechanism of the RIPs, their magnetic parameters, and their behavior at low magnetic fields. We will describe them in this order.

3.1. Assignment of the Reaction Intermediates. MPTZ and DCNB are the typical electron donor and acceptor, respectively, in photochemical reactions. There is, however, no precedent study on their reaction, but an electron transfer is expected from excited MPTZ to ground-state DCNB. The transient optical absorption spectrum observed immediately after excitation of a 2-PrOH solution of MPTZ (1×10^{-3} mol dm^{-3}) and DCNB (1×10^{-3} mol dm^{-3}) has a peak around 460 nm, which is ascribed to the triplet excited state of MPTZ (^{3}MPTZ*).[20,21] The spectrum observed at 400 ns after excitation has two peaks around 430 and 520 nm. The former is attributed to the radical anion of DCNB (DCNB$^{\bullet-}$)[22] and the latter to the radical cation of MPTZ (MPTZ$^{\bullet+}$).[20,21] Similar spectra were observed for the solution of MPTZ (1×10^{-3} mol dm^{-3}) and F_4DCNB (1×10^{-3} mol dm^{-3}) except for the absence of the spectrum of DCNB$^{\bullet-}$. The peak observed around 390 nm after several hundred nanoseconds instead of DCNB$^{\bullet-}$ may be attributed to the radical anion of F_4DCNB (F_4DCNB$^{\bullet-}$). Similar spectra were also obtained in benzene−DMSO (3:1, v/v) solutions[23] of MPTZ + DCNB and MPTZ + F_4DCNB and in a micellar Brij35 (5×10^{-2} mol dm^{-3}) solution of MPTZ + DCNB. Consequently, we can safely describe these photochemical reactions as follows:

$$\text{MPTZ} \xrightarrow{h\nu} {}^1\text{MPTZ}^* \rightarrow {}^3\text{MPTZ}^* \quad (1)$$

$${}^3\text{MPTZ}^* + (\text{F}_4)\text{DCNB} \rightarrow {}^3[\text{MPTZ}^{\bullet+}\ (\text{F}_4)\text{DCNB}^{\bullet-}] \quad (2)$$

$${}^3[\text{MPTZ}^{\bullet+}\ (\text{F}_4)\text{DCNB}^{\bullet-}] \leftrightarrow {}^1[\text{MPTZ}^{\bullet+}\ (\text{F}_4)\text{DCNB}^{\bullet-}] \quad (3)$$

$${}^1[\text{MPTZ}^{\bullet+}\ (\text{F}_4)\text{DCNB}^{\bullet-}] \rightarrow \text{MPTZ} + (\text{F}_4)\text{DCNB} \quad (4)$$

$${}^{1,3}[\text{MPTZ}^{\bullet+}\ (\text{F}_4)\text{DCNB}^{\bullet-}] \rightarrow \text{MPTZ}^{\bullet+} + (\text{F}_4)\text{DCNB}^{\bullet-} \quad (5)$$

Here, ^{1}[ ] and ^{3}[ ] represent singlet and triplet RIPs. There are decay processes of escaped radical ions after their formation, reaction 5, which will be discussed later. We have measured the rate of reaction 2. The quenching rates by DCNB were 4.3 $\times$ 10^9 and 4.6 $\times$ 10^9 mol^{-1} dm^3 s^{-1} in the 2-PrOH and benzene−DMSO solutions, respectively. Those by F_4DCNB were 5.9 $\times$ 10^9 and 8.6 $\times$ 10^9 mol^{-1} dm^3 s^{-1} in the 2-PrOH and benzene−DMSO solutions, respectively. These errors are less than ±10%.

Time-resolved ESR spectra are also measured for these reactions. The CIDEP spectra observed at a delay time of 500 ns after excitation of a 2-PrOH solution of MPTZ (1×10^{-3} mol dm^{-3}) and DCNB (1×10^{-3} mol dm^{-3}) are shown in Figure 1A. A similar one was observed with F_4DCNB (1×10^{-3} mol dm^{-3}) as shown in Figure 1B. Both spectra have three broad absorptive peaks in lower fields and several sharp emissive peaks in higher fields. The broad ones are well reproduced by the hyperfine coupling (hfc) constants of MPTZ$^{\bullet+}$ ($g = 2.0050$, $a_N = 0.765$ mT, $a_H = 0.742 \times 3$, 0.213×2, 0.113×2, 0.070×2, 0.023 mT $\times 2$).[24] The sharp ones in Figure 1A are well reproduced by the hfc constants of DCNB$^{\bullet-}$ ($g = 2.0013$ relative to MPTZ$^{\bullet+}$, $a_N = 0.181$ mT $\times 2$, $a_H = 0.159$ mT $\times 4$).[25] In comparison with those of DCNB$^{\bullet-}$, the sharp ones in Figure 1B are ascribed to F_4DCNB$^{\bullet-}$ ($g = 2.0012$ relative to MPTZ$^{\bullet+}$, $a_N = 0.206$ mT $\times 2$, $a_F = 0.206$ mT $\times 4$). The hfc constants of F_4DCNB$^{\bullet-}$ and the g values of both dicyanobenzenes were obtained in this work for the first time.

Although the assignment of F_4DCNB$^{\bullet-}$ is straightforward, the hfc constant of the F atoms is only a little larger than that of the H atoms of DCNB$^{\bullet-}$. In the case of fluorinated aromatic anions, the hfc constants of the F atoms are various. The hfc constant of the hexafluorobenzene anion is 40 times larger than that of the benzene anion.[26] On the other hand, the hfc constant of F atoms in the *p*-difluorobenzene anion is one-third of the H atoms in the same anion.[26] Therefore, a little larger hfc constant of the F atoms in F_4DCNB$^{\bullet-}$ than that of the H atoms in DCNB$^{\bullet-}$ may not be surprising. This resemblance of the hfc constants and g values between DCNB$^{\bullet-}$ and F_4DCNB$^{\bullet-}$ is accidental but useful for the comparison of their MFEs.

The A/E phase patterns of the observed CIDEP spectra shown in Figure 1A and 1B can be explained by the radical pair mechanism due to singlet RPs with $J < 0$ or due to triplet RPs with $J > 0$. Here, J is the exchange integral. Transient optical absorption spectra clearly show that these reactions originated from ^{3}MPTZ*. Consequently, J is concluded to be positive in these reactions. Although J is usually negative in the cases of neutral RPs, there are several reports showing positive J values in RIP reactions.[27,28]

3.2. Magnetic Field Effects at 0−1.75 T. The MFEs of the photoinduced electron-transfer reactions between ^{3}MPTZ* and (F_4)DCNB were measured at 0−1.75 T using the electromagnet. The time profiles of the transient absorbance, $A(t)$, for the reaction of ^{3}MPTZ* and DCNB in 2-PrOH were measured at 520 nm. Among the observed $A(t)$ curves, those obtained at $B = 0$, 10, 500, and 1500 mT are shown in Figure

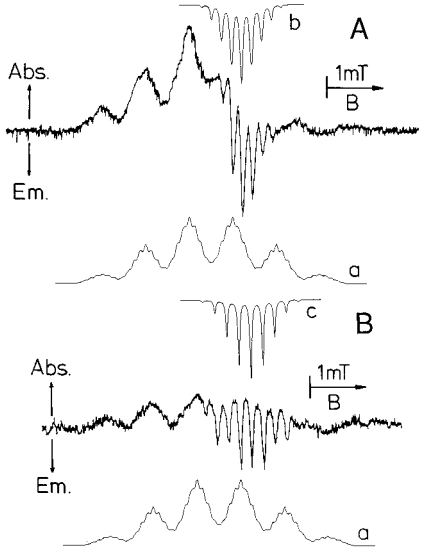

Figure 1. Time-resolved X-band ESR spectra observed at a delay of 0.5 μs after excitation of (A) the 2-PrOH solutions of MPTZ (1×10^{-3} mol dm^{-3}) and DCNB (1×10^{-3} mol dm^{-3}) and (B) the 2-PrOH solution of MPTZ (1×10^{-3} mol dm^{-3}) and F_4DCNB (1×10^{-3} mol dm^{-3}). The simulated spectra of (a) MPTZ$^{\bullet+}$, (b) DCNB$^{\bullet-}$, and (c) F_4DCNB$^{\bullet-}$ are also shown.

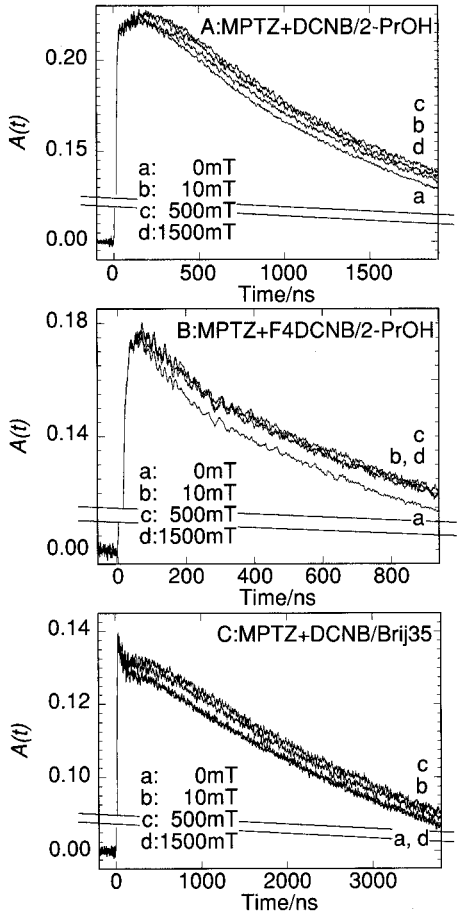

Figure 2. Time profiles of the transient absorbance, $A(t)$, curves observed at 520 nm of (A) the 2-PrOH solution of MPTZ (1×10^{-3} mol dm^{-3}) and DCNB (1×10^{-3} mol dm^{-3}), (B) the 2-PrOH solution of MPTZ (1×10^{-3} mol dm^{-3}) and F_4DCNB (1×10^{-3} mol dm^{-3}), and (C) the micellar Brij35 solution of MPTZ (1×10^{-3} mol dm^{-3}) and DCNB (1×10^{-3} mol dm^{-3}). The applied magnetic fields are described in the figures.

2A. Each $A(t)$ curve is composed of a rise from 0 to *ca.* 200 ns and a decay afterwards. In the presence of a magnetic field of 10 or 500 mT, the rise part is enhanced in comparison with that at 0 mT. At 200 ns, the difference is clear, and this difference seems to increase up to 500 ns. In the presence of the fields larger than 500 mT, the rise part became smaller than that at 500 mT, as shown by the $A(t)$ curve at 1500 mT. The decay process afterwards was found to proceed bimolecularly.

Since the bimolecular decay is only expected for uncorrelated species, the collapse of the geminate RIP is expected to be terminated before this bimolecular decay. Consequently, we can conclude that the rise part includes the formation and collapse of the geminate RIP. This means that reactions 2−5 proceed simultaneously. The enhancement of the rise part comes from the increase of escaped MPTZ$^{\bullet+}$ in reaction 5, which is induced by the decrease of recombination of the geminate RIP in reaction 4. This means that the T−S (triplet−singlet) conversion of the geminate RIP in reaction 3 is blocked at $B \leq 500$ mT and then accelerated at $B \geq 500$ mT.

Similarly, $A(t)$ curves for the reaction of ^{3}MPTZ* and F_4-DCNB in 2-PrOH were measured at 520 nm, and several curves are shown in Figure 2B. Since MPTZ$^{\bullet+}$ is common in the reactions of this paper, we chose its peak at 520 nm for comparing the MFEs under different conditions. Each $A(t)$ curve is composed of a rise from 0 to *ca.* 60 ns and a decay afterwards. This rise is faster than that of DCNB. This is due to a larger quenching rate of F_4DCNB than that of DCNB. In the presence of a magnetic field, the rise part is also enhanced as in the case of DCNB. The main effect appears, however, at the initial decay part up to 200 ns. Therefore, the decay part of this reaction is composed of the geminate recombination at the initial part and the random recombination of the escaped radical ions afterwards.

Since reactions 2−5 proceed almost simultaneously, we could not derive each reaction rate directly from the $A(t)$ curves observed in the reaction of ^{3}MPTZ* and DCNB in 2-PrOH. From the $A(t)$ curves in that of ^{3}MPTZ* and F_4DCNB in 2-PrOH, we could observe the decay of the geminate RIP, but its separation from the RIP formation is not complete. From a rough estimation, the recombination rate of the RIP at 0 mT was determined to be 1×10^7 s^{-1}. In the presence of fields, the RIP decay became too unclear to obtain the rate. The increase of quencher concentration, on the other hands, involves many difficulties as follows:

(1) The degenerate electron-transfer reactions[29] between cyanobenzenes and their anions may modify the observed MFEs. This process is very interesting but is beyond the scope of this paper.

(2) A charge-transfer complex between MPTZ and (F_4)DCNB may be formed at higher concentrations. This may give completely different results. At the present concentration, there is no evidence for the formation of such complexes.

(3) The solubility of cyanobenzenes in organic solvents and micellar solutions is generally low. We may not dissolve them enough to separate reaction 2 from others, especially in micellar solutions.

Therefore, we chose dilute solutions to avoid any additional effects on the MFEs at the first stage.

$A(t)$ curves for the reaction of ^{3}MPTZ* and DCNB in Brij35 micellar solution were measured at 520 nm, and some of them in the absence and presence of magnetic fields are shown in Figure 2C. Each $A(t)$ curve is composed of a decay from 0 to *ca.* 200 ns, a rise up to *ca.* 500 ns, and then a decay afterwards. The MFEs are observed at the rise part. It is obvious that the observed reaction is not homogeneous since the decay and rise rates in the $A(t)$ curves do not correspond to each other. Although the $A(t)$ curves are composed of independent dynam-

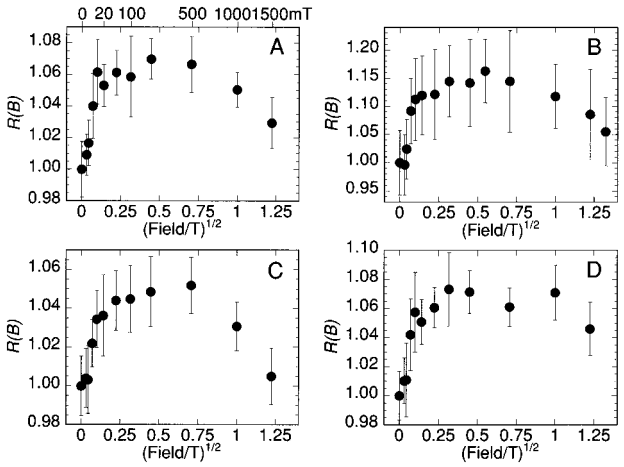

Figure 3. Magnetic field dependence of $R(B) = A(1\ \mu s, B)/A(1\ \mu s, 0\ T)$ values in the reactions of (A) the 2-PrOH solution of MPTZ (1×10^{-3} mol dm^{-3}) and DCNB (1×10^{-3} mol dm^{-3}), (B) the benzene−DMSO (3:1, v/v) solution of MPTZ and DCNB, (C) the micellar Brij35 solution of MPTZ and DCNB, and (D) the 2-PrOH solution of MPTZ (1×10^{-3} mol dm^{-3}) and F_4DCNB (1×10^{-3} mol dm^{-3}).

ics, the MFE of the rise part is reasonably ascribed to the same reaction scheme as in 2-PrOH solutions.

The plot of $A(t)$ values at 520 nm after the complete collapse of the geminate RIP against the magnetic field should show the MFE on the yield of escaped MPTZ$^{\bullet+}$ from the geminate RIP.[18] In order to make such a plot, we took the delay time to be around 1 μs since we found small MFEs on the bimolecular decay rates of escaped radical ions. The bimolecular decay rates of the reactions of ^{3}MPTZ* and (F_4)DCNB in 2-PrOH were found to decrease with increasing B from 0 to 500 mT and then to increase with increasing B from 500 to 1500 mT. This effect will be discussed later with the results obtained at $B = 0-10$ T.

To compare the MFEs of the reactions of ^{3}MPTZ* and DCNB in 2-PrOH, benzene−DMSO (3:1, v/v), and micellar Brij35 solutions, we plotted the relative MFE of $A(1\ \mu s)$ at 520 nm, $R(B) = A(1\ \mu s, B)/A(1\ \mu s, 0\ T)$, against the square root of the field strength, $B^{1/2}$, in Figure 3A−C. In Figure 3D, we plotted the $R(B)$ values obtained at $t = 0.8\ \mu s$ in the reaction of ^{3}MPTZ* and F_4DCNB in 2-PrOH, since the observed time region was up to 940 ns. In each reaction, the $R(B)$ value increases quickly with increasing B from 0 to 20 mT, attains a plateau at around 500 mT, and then starts to decrease with increasing B above 500 mT. Since the generated RIP, ^{3}[MPTZ$^{\bullet+}$ DCNB$^{\bullet-}$], is common in Figure 3A−C, the magnetic field dependencies in the figures are similar to each other irrespective of the solvents as expected. The magnetic parameters of DCNB$^{\bullet-}$ and F_4DCNB$^{\bullet-}$ are also similar to each other. Consequently, the magnetic field dependencies of these RIPs are also expected to be similar as shown in Figure 3A and 3D. A detailed comparison between DCNB and F_4DCNB will be discussed later with the results obtained at $B = 0-10$ T.

The steep rises at low fields in the results shown in Figure 3A−D are expected to be due to the hfc mechanism.[2] If we assume that the average of the $R(B)$ values from 100 to 500 mT is the maximum effect, the B_{half} field where half of the maximum effect appears is calculated to be 4.0, 4.3, 5.8, and 4.2 mT for the results shown in Figure 3A−D. The semiclassical estimation of the B_{half} field is given as follows:[30]

$$B_{half} = 2(B_{MPTZ^{\bullet+}}{}^2 + B_{(F_4)DCNB^{\bullet-}}{}^2)/(B_{MPTZ^{\bullet+}} + B_{(F_4)DCNB^{\bullet-}}) \quad (6)$$

where $B_{radical} = (\Sigma_j I_j(I_j + 1)a_j{}^2)^{1/2}$. The value for [MPTZ$^{\bullet+}$ DCNB$^{\bullet-}$] is 2.7 mT and that for [MPTZ$^{\bullet+}$ F_4DCNB$^{\bullet-}$] is 2.6 mT. Concerning the experimental errors and used assumptions, we can see that the agreement between the observed and estimated B_{half} values is good.

Although the magnetic field dependencies observed in the above reactions are similar to each other, their magnitudes are varied by their environments. In the case of ^{3}[MPTZ$^{\bullet+}$ DCNB$^{\bullet-}$], the maximum $R(B)$ values are 1.070, 1.163, and 1.052 in 2-PrOH, benzene−DMSO, and micellar Brij35 solutions, respectively. It is clear that the nonionic micellar environment of Brij35 does not improve the magnitude of the MFEs. It is well-known that the micellar environments enhance the MFEs in many reactions of neutral RPs.[1] On the other hand, anionic or cationic micelles such as sodium dodecyl sulfate or hexadecyltrimethylammonium chloride are accepted to be an excellent circumstance for the charge separation[31] where the geminate recombination of RIP, hence its MFE, is very small. We can avoid this effect by using nonionic micelles. The main enhancement of the MFE in micellar solutions, however, comes from the hydrophobic confinement of the RPs, which may not be expected for ionic species such as RIPs. Consequently, the present result indicates that the nonionic micelle of Brij35 has neither positive nor negative effects for confinement of RIPs. The complicated kinetic behavior in Figure 2C also indicates that the micellar solution is not a good environment for detailed studies of the MFEs of RIPs.

From our experience, 2-PrOH is a special solvent in which many reactions show the maximum MFEs among homogeneous single solvents. We have found, however, in this study that the MFEs in benzene−DMSO are larger than those in 2-PrOH. There are several papers reporting that the binary mixture of polar and nonpolar solvents sometimes enhances the MFEs of RIPs.[23,32,33] The ionic or very polar species in such a solvent is surrounded by polar solvent molecules. Since the RIP generated in a cluster is confined in it, the MFE is expected to be enhanced as is in the reversed micellar solutions.[34] The bimolecular decay of RIPs in benzene−DMSO shows that the confinement by polar solvent molecules is not permanent but enough to enhance the recombination.

Since MPTZ and DCNB are a good electron donor and acceptor, respectively, they have been used separately for the studies of MFEs of RIPs. The chained derivatives of MPTZ with methyl viologen were applied for the studies of biradical ion pairs.[35] Many efforts were devoted for the combination of pyrene and DCNB.[30,36] DCNB was also applied for the photoisomerization of olefins.[37] These studies were carried out under low magnetic fields as mentioned in this section, but there has been no study at fields larger than 1.1 T.[37]

3.3. Magnetic Field Effects at 0−10 T. To elucidate the MFE of RIPs in homogeneous solutions under fields larger than 1.75 T, the reactions of ^{3}MPTZ* with DCNB and F_4DCNB were investigated in 2-PrOH and benzene−DMSO (3:1, v/v) solutions. We have observed similar kinetic behavior of RIPs in the high field region ($B = 1.75-10$ T) to that in the low one ($B \leq 1.75$ T). Instead of the reproduction of the $A(t)$ curves, we show the $1/A(t)$ curves obtained in the reaction of ^{3}MPTZ* and F_4DCNB in 2-PrOH in Figure 4A. The results of the other reactions gave similar figures except for their rates. A linear $1/A(t)-t$ relationship shown in Figure 4A is described by a bimolecular decay process of escaped radical ions. As clearly seen in this figure, the decay process later than 1.5 μs after excitation is almost completely described by the bimolecular process and the bimolecular decay rate is dependent on B, as mentioned earlier. In Figure 4B and 4C, we show observed MFEs on the bimolecular decay rates (k/ϵ) of the reactions in

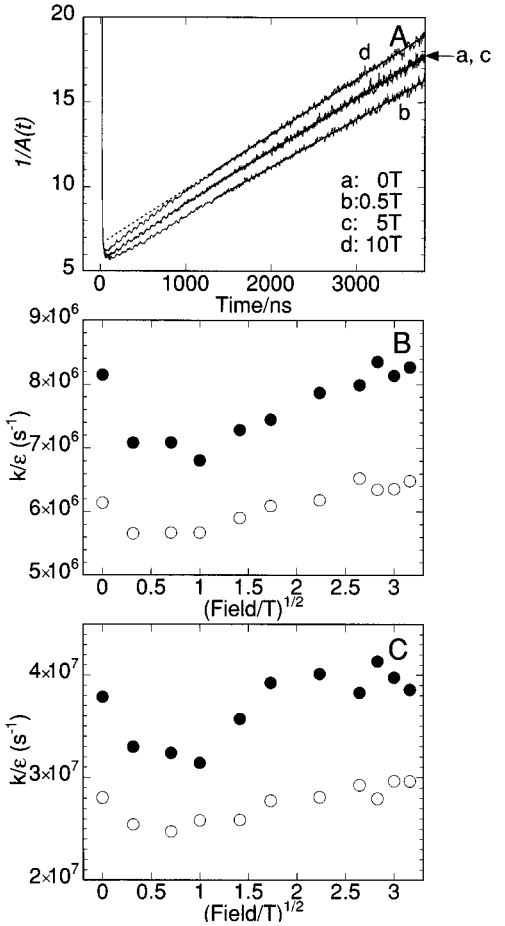

Figure 4. (A) $1/A(t)$ curves observed at 520 nm of the 2-PrOH solution of MPTZ (1×10^{-3} mol dm^{-3}) and F_4DCNB (1×10^{-3} mol dm^{-3}) in the absence and presence of magnetic fields. (B) Magnetic field dependence of the bimolecular decay rates in the 2-PrOH solutions of (●) MPTZ (1×10^{-3} mol dm^{-3}) with DCNB (1×10^{-3} mol dm^{-3}) and (○) MPTZ (1×10^{-3} mol dm^{-3}) with F_4DCNB (1×10^{-3} mol dm^{-3}). (C) Magnetic field dependence of the bimolecular decay rates in the benzene−DMSO (3:1, v/v) solutions of (●) MPTZ with DCNB and (○) MPTZ with F_4DCNB.

2-PrOH and benzene−DMSO, respectively. We can estimate from Figure 4A the errors of k/ϵ to be less than ±3%. As seen from these figures, the bimolecular decay rates decrease with increasing B from 0 to 0.5 T and then start to increase above it. The rates at 10 T are slightly larger than those at 0 T. The rates of F_4DCNB are smaller than those of DCNB.

These bimolecular reactions can be described by the reencounter of radical ions, reaction 5′, and by reactions 3 and 4 as follows:

$$\mathrm{MPTZ}^{\bullet+} + (\mathrm{F_4})\mathrm{DCNB}^{\bullet-} \xrightarrow{75\%} {}^3[\mathrm{MPTZ}^{\bullet+}\ (\mathrm{F_4})\mathrm{DCNB}^{\bullet-}] \quad (5')$$

$$\xrightarrow{25\%} {}^1[\mathrm{MPTZ}^{\bullet+}\ (\mathrm{F_4})\mathrm{DCNB}^{\bullet-}] \quad (5')$$

$${}^3[\mathrm{MPTZ}^{\bullet+}\ (\mathrm{F_4})\mathrm{DCNB}^{\bullet-}] \leftrightarrow {}^1[\mathrm{MPTZ}^{\bullet+}\ (\mathrm{F_4})\mathrm{DCNB}^{\bullet-}] \quad (3)$$

$${}^1[\mathrm{MPTZ}^{\bullet+}\ (\mathrm{F_4})\mathrm{DCNB}^{\bullet-}] \rightarrow \mathrm{MPTZ} + (\mathrm{F_4})\mathrm{DCNB} \quad (4)$$

Since reaction 3 is influenced by magnetic fields, the bimolecular decay process may also be influenced by them as observed. The random reencounter of escaped radical cation and anion, reaction 5′, forms statistically triplet and singlet RIPs in a 3:1 ratio. Thus, the MFEs on the reactions of escaped radical ions should qualitatively be the same as those of triplet-born geminate RIPs. The decrease in the recombination rates with increasing B from 0 to 0.5 T and the increase above it should also be observed in the geminate RIPs. Although it was hard to directly observe the MFEs on the geminate recombination rates as described earlier, we could detect the MFEs on the yield of escaped $\mathrm{MPTZ}^{\bullet+}$ at $B = 0-10$ T.

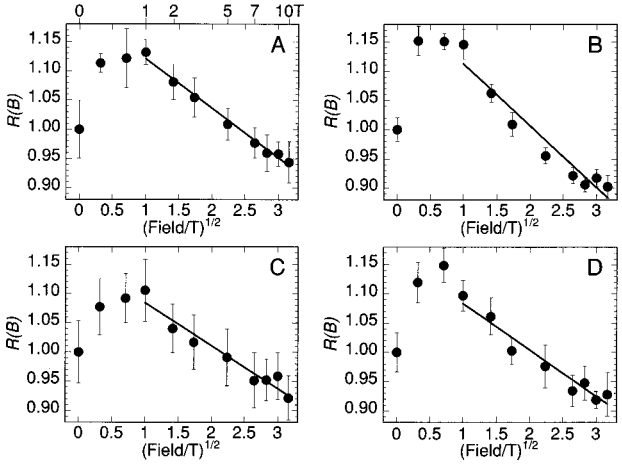

Figure 5. Magnetic field dependence of the $R(B)$ values of (A) the 2-PrOH solution of MPTZ (1×10^{-3} mol dm^{-3}) and DCNB (1×10^{-3} mol dm^{-3}), (B) the benzene−DMSO (3:1, v/v) solution of MPTZ and DCNB, (C) the 2-PrOH solution of MPTZ (1×10^{-3} mol dm^{-3}) and F_4DCNB (1×10^{-3} mol dm^{-3}), and (D) the benzene−DMSO (3:1, v/v) solution of MPTZ and F_4DCNB. The solid lines are the least-squares fitted lines with the data at $B = 1-10$ T.

The $R(B) = A(1\ \mu\mathrm{s}, B)/A(1\ \mu\mathrm{s}, 0\ \mathrm{T})$ values of the reactions of ^{3}MPTZ* and (F_4)DCNB in 2-PrOH and benzene−DMSO in the absence and presence of the magnetic fields are plotted against $B^{1/2}$ in Figure 5A−D, respectively. It is noteworthy that the $1/A(t)$ plot exaggerates the tail parts of the $A(t)$ curves and also the differences of their decay rates. If the MFE due to the bimolecular process is large enough, the tail parts of the $A(t)$ curves should separate to each other with increasing t like the $1/A(t)$ curves in Figure 4A. On the contrary, the tail parts of the $A(t)$ curves are practically parallel to each other as shown in Figure 2A and 2B. This fact suggests that the contribution of the MFE due to the escaped radical ions is small. Consequently, we can safely regard the $R(B)$ values as a measure of the MFE of the geminate RIPs, although we cannot eliminate the contribution of the MFEs due to escaped radical ions from them. We plotted an extrapolation of the fitting line at 10 T in Figure 4A. This deviation means that the recombination rate of the geminate RIP is significantly larger than the bimolecular decay rate. On the other hand, the extrapolation at 0.5 T is almost the same as the $A(t)$ curve. This difference of the $A(t)$ curves at 0.5 and 10 T originates from the MFE of the geminate RIPs.

As shown in Figure 5, $R(B)$ increases with increasing B from 0 to 0.5 T and then starts to decrease with increasing B from 0.5 to 10 T. In the reactions in 2-PrOH (Figure 5A and 5C), $R(5\ \mathrm{T})$'s are similar to $R(0\ \mathrm{T})$'s irrespective of the electron acceptors. The overlap of the $A(t)$ curves at 0 and 5 T in Figure 4A confirms this fact. In benzene−DMSO (Figure 5B and 5D), $R(3\ \mathrm{T})$'s are similar to $R(0\ \mathrm{T})$'s. Above these fields, $R(B)$ values are smaller than $R(0\ \mathrm{T})$'s. The decrease of $R(B)$ above 1 T seems linear to $B^{1/2}$, especially for the reactions in 2-PrOH. In Figure 5, we plotted-least-squares-fitted lines at $B = 1-10$ T.

There are two possible mechanisms to explain the MFEs in the high-field region. One of them is the ΔgM,[6] and the other is the relaxation mechanism.[10,38] The observed linear relationship between $R(B)$ and $B^{1/2}$ can be interpreted by the ΔgM as

described below. It is noteworthy that the smaller $R(B)$ values observed in the high-field region than $R(0\ \mathrm{T})$ cannot be explained by the relaxation mechanism.[39] If we use the assumptions described in refs 3 and 6, the theoretical expression of the MFE due to the ΔgM on the relative yield ($Y_{\Delta g\mathrm{M}}$) of the escaped radical from a triplet RP is as follows;

$$Y_{\Delta g\mathrm{M}}(B) - 1 = -{}^1/_3(\lambda m/(1-p))(\pi\Delta g\beta B/2)^{1/2} \qquad (7)$$

Here, λ ($0 \le \lambda \le 1$) is the recombination probability of the singlet RP at its reencounter. m and p ($0.5 \le p < 1$) are the factors appearing in the reencounter function given by Noyes.[40,41] By replacing $\lambda m/3(1-p)$ with m/p, we get the expression for the yield of cage products from a singlet RP.[5] The reencounter function is based on the noninteracting species such as neutral RPs. Since the Coulombic attraction between RIPs at large separation becomes negligible in polar solution, eq 7 can be tentatively applicable to the RIP reactions. In order to describe the dynamic behavior of RIPs quantitatively, we had better use a numerical method such as the procedure derived by Pedersen.[42]

The experimental $R(B) = A(1\ \mu\mathrm{s}, B)/A(1\ \mu\mathrm{s}, 0\ \mathrm{T})$ values include the contribution of the MFE due to the hfc mechanism (HFCM), but the conversion to the $Y_{\Delta g\mathrm{M}}(B)$ values is simply to multiply $R(B)$ by a constant. We can safely assume a certain magnetic field, B_0, where the MFE due to the HFCM is terminated and the MFE due to the ΔgM is negligible. Experimentally, B_0 is considered to be 0.1−0.5 T. By using $A(1\ \mu\mathrm{s}, B_0)$ as the reference, we can get the $Y_{\Delta g\mathrm{M}}(B)$ value, as follows:

$$\begin{aligned} Y_{\Delta g\mathrm{M}}(B) &= A(1\,\mu\mathrm{s}, B)/A(1\,\mu\mathrm{s}, B_0) \\ &= A(1\,\mu\mathrm{s}, B)/A(1\,\mu\mathrm{s}, 0\,\mathrm{T}) \times A(1\,\mu\mathrm{s}, 0\,\mathrm{T})/A(1\,\mu\mathrm{s}, B_0) \\ &= R(B)/R(B_0) \end{aligned} \qquad (8)$$

Since the observed $R(B)$ values, and hence the $Y_{\Delta g\mathrm{M}}(B)$ values, above 1 T are practically proportional to $B^{1/2}$, we can safely conclude that the MFEs of the present reactions at $B = 0.5-10$ T are due to the ΔgM.

According to eq 7, the $\lambda m/(1-p)$ value is a good parameter to compare the MFEs of many triplet reactions, removing the difference in Δg values. By this value, we can compare other conditions than the Δg value which affect the magnitude of the MFEs. In order to compare the MFEs of the singlet and triplet reactions, we must compare m/p and $\lambda m/(1-p)$. For a simple comparison of the magnitude of MFEs, we can compare these values directly because these values are derived from the observed MFEs and the Δg values in the same manner.

To obtain the experimental $\lambda m/(1-p)$ values, we took B_0 to be 0.1 T to avoid overestimation because the larger B_0 field gives the larger values. We used the extrapolated $R(0.1\ \mathrm{T})$ values obtained from the linear fitting at $B = 1-10$ T instead of the observed ones to avoid the fluctuation of the $\lambda m/(1-p)$ values due to the single experimental errors at 0.1 T. By this procedure, we obtained the $\lambda m/(1-p)$ values to be 9.5×10^{-6} and 1.2×10^{-5} $\mathrm{s}^{1/2}$, in the reactions of ^{3}MPTZ* and DCNB in 2-PrOH and benzene−DMSO, respectively. Those of ^{3}MPTZ* and F_4DCNB are 8.5×10^{-6} and 9.1×10^{-6} $\mathrm{s}^{1/2}$, respectively. In the hydrogen abstraction from *p*-aminothiophenol by the triplet excited state of xanthone in a sodium dodecyl sulfate micelle, we observed MFEs due to the ΔgM of a neutral RP consisting of xanthone ketyl and *p*-aminophenylthiyl radicals.[43] In this reaction, we can calculate the $\lambda m/(1-p)$ value to be 1.5×10^{-5} $\mathrm{s}^{1/2}$. In the case of the singlet photodecomposition reaction of dibenzoyl peroxide in toluene, the MFEs due to the ΔgM of a neutral RP consisting of benzoyloxy and phenyl radicals were observed.[5] The m/p value of this reaction, instead of $\lambda m/(1-p)$, is calculated to be 1.08×10^{-6} $\mathrm{s}^{1/2}$.[3,6]

The experimental conditions of the above reactions are quite different from each other. Consequently, we should not discuss λ, m, and p separately but compare simply the $\lambda m/(1-p)$ or m/p values as the measure of the magnitude of their MFEs removing the difference in Δg values. It is obvious that the MFEs of the RIPs are much larger than that of the neutral RP in homogeneous solution. This difference is easily attributed to the confinement of the RIPs due to the Coulombic attraction which is absent in the neutral RP in homogeneous solution. The comparison also reveals that the micellar solution is an excellent environment for the enhancement of the MFE of the RPs. The Coulombic attraction between the RIPs in homogeneous solutions is, in fact, not so inferior to the micellar confinement for the enhancement of the MFEs.

In the comparison of DCNB and F_4DCNB, we can discuss it in detail, since the parameters to describe their reactions should be similar to each other. The $\lambda m/(1-p)$ values indicate that the MFEs in the reactions of ^{3}MPTZ* and F_4DCNB are somewhat smaller than those of ^{3}MPTZ* and DCNB. Since the contribution of the Δg value is removed from the $\lambda m/(1-p)$ value, the difference comes from other conditions. The remaining factor to determine the magnitude of the MFE is the competition between recombination, reaction 4, and escape of singlet RIP, reaction 5, which is depicted by λ. A smaller λ can be explained by a larger escaping rate and/or by a smaller recombination rate. The bimolecular decay rate of escaped radical ions is also affected by this competition. The bimolecular decay rates of $MPTZ^{\bullet+}$ and $F_4DCNB^{\bullet-}$ are found to be smaller than those of $MPTZ^{\bullet+}$ and $DCNB^{\bullet-}$. This implies that the λ value of $MPTZ^{\bullet+}$ and $F_4DCNB^{\bullet-}$ is smaller than that of $MPTZ^{\bullet+}$ and $DCNB^{\bullet-}$. The escaping rate of $F_4DCNB^{\bullet-}$ might be even smaller because the molecular size of $F_4DCNB^{\bullet-}$ must be a little larger than that of $DCNB^{\bullet-}$. Accordingly, we can conclude that the recombination rate of $^1[MPTZ^{\bullet+}\ F_4DCNB^{\bullet-}]$ is slower than that of $^1[MPTZ^{\bullet+}\ DCNB^{\bullet-}]$.

Since the studies by Marcus[44] and Rehm−Weller,[45] there have been many studies to combine the reaction rates and the free-energy changes of the reactions. Applying the triplet energy of MPTZ (2.64 eV),[20] the oxidation potential of MPTZ (0.64 eV),[46] and the reduction potential of DCNB (−1.6 eV),[47] the free-energy changes of the forward (f) and backward (b) reactions are calculated to be $\Delta G_\mathrm{f} = -0.40 - C$ eV and $\Delta G_\mathrm{b} = -2.24 + C$ eV for the reaction of ^{3}MPTZ* and DCNB, respectively. Here, C (∼0.1 eV) is a Coulombic attraction term between radical ions. The reduction potential of F_4DCNB has not been measured. If we substitute it by the reduction potential of tetrafluoro-1,2-dicyanobenzene (−1.21 eV),[48] we get $\Delta G_\mathrm{f} = -0.79 - C$ eV and $\Delta G_\mathrm{b} = -1.85 + C$ eV, respectively. The magnitude of ΔG_f implies that the quenching rate of ^{3}MPTZ* by F_4DCNB should be larger than that by DCNB, which corresponds to our observation. For the back-electron-transfer reactions, the inverted region is sometimes observed. The smaller back-electron-transfer rate in F_4DCNB indicates that the maximum point of the bell-shape dependence is not larger than $-1.85 + C$ eV.

By means of the nanosecond laser photolysis, the magnetic field effects on the photochemical electron-transfer reactions from the triplet excited state of 10-methylphenothiazine to 1,4-dicyanobenzene or its tetrafluoro derivative are investigated. They showed the magnetic field effects due to the hyperfine coupling mechanism at low fields ($B = 0-0.5$ T) and those due to the Δg mechanism at high fields ($B < 10$ T). The micellar solution is found to be unsuitable for the confinement

of radical ion pairs. On the contrary, the binary solution of polar and nonpolar solvents is confirmed to be a better condition for that purpose. The comparison of $\lambda m/(1-p)$ values indicates that the confinement of radical ion pair in a binary solution is not so inferior to that of neutral RP in micellar solutions. A little smaller magnitude of the magnetic field effects of the fluorinated derivative than those of the 1,4-dicyanobenzene is originated from its smaller charge recombination rate than the nonsubstituted one. This may be due to its smaller free-energy change in the back-electron-transfer process.

The low solubility of organic compounds into aqueous micellar solutions is the main difficulty of the practical application of the magnetic field effect of RPs. The RIP reactions in homogeneous binary solutions are another candidate. It is very interesting to investigate the free-energy dependence of the magnetic field effects of RIPs. This may provide new insight into photochemical electron-transfer reactions. We already found the magnetic field effects with other cyanobenzenes such as 1,2-dicyanobenzene. The expansion in this direction is now in progress.

Acknowledgment. Y. S. thanks support by a Grant-in-Aid for Scientific Research (07804037) from the Ministry of Education, Science and Culture, Japan.

References and Notes

(1) Steiner, U. E.; Ulrich, T. *Chem. Rev.* **1989**, *89*, 51.
(2) Hayashi, H.; Sakaguchi, Y. *Lasers in Polymer Science and Technology: Applications*; CRC: Boca Raton, FL, 1990; Vol. 2, Chapter 1.
(3) Hayashi, H. *Photochemistry and Photophysics*; CRC: Boca Raton, FL, 1990; Vol. 1, Chapter 2.
(4) Hayashi, H.; Itoh, K.; Nagakura, S. *Bull. Chem. Soc. Jpn.* **1966**, *39*, 199. Itoh, K.; Hayashi, H.; Nagakura, S. *Mol. Phys.* **1969**, *17*, 561.
(5) Tanimoto, Y.; Hayashi, H.; Nagakura, S.; Sakuragi, H.; Tokumaru, K. *Chem. Phys. Lett.* **1976**, *41*, 267.
(6) Hayashi, H.; Nagakura, S. *Bull. Chem. Soc. Jpn.* **1978**, *51*, 2862.
(7) Sakaguchi, Y.; Hayashi, H.; Nagakura, S. *Bull. Chem. Soc. Jpn.* **1980**, *53*, 39.
(8) Sakaguchi, Y.; Nagakura, S.; Hayashi, H. *Chem. Phys. Lett.* **1980**, *72*, 420. Hayashi, H.; Sakaguchi, Y.; Nagakura, S. *Chem. Lett.* **1980**, 1149.
(9) Sakaguchi, Y.; Nagakura, S.; Hayashi, H. *Chem. Phys. Lett.* **1984**, *106*, 420. Sakaguchi, Y.; Hayashi, H. *Chem. Phys.* **1992**, *162*, 119.
(10) Hayashi, H.; Nagakura, S. *Bull. Chem. Soc. Jpn.* **1984**, *57*, 322.
(11) Sakaguchi, Y.; Hayashi, H.; Murai, H.; I'Haya, Y. J. *Chem. Phys. Lett.* **1984**, *110*, 275. Sakaguchi, Y.; Hayashi, H.; Murai, H.; I'Haya, Y. J.; Mochida, K. *Chem. Phys. Lett.* **1985**, *120*, 401.
(12) Buckley, C. D.; Hunter, D. A.; Hore, P. J.; McLauchlan, K. A. *Chem. Phys. Lett.* **1987**, *135*, 307.
(13) Closs, G. L.; Forbes, M. D. E.; Norris, J. R., Jr. *J. Phys. Chem.* **1987**, *91*, 3592.
(14) Sakaguchi, Y.; Hayashi, H. *Chem. Lett.* **1993**, 1183.
(15) Sakaguchi, Y.; Hayashi, H. Manuscript in preparation.
(16) Hayashi, H.; Wakasa, M.; Sakaguchi, Y. *J. Chin. Chem. Soc.* **1995**, *42*, 343.
(17) Steiner, U. *Z. Naturforsch.* **1979**, *34a*, 1093.
(18) Sakaguchi, Y.; Hayashi, H. *J. Phys. Chem.* **1984**, *88*, 1437.
(19) Sakaguchi, Y.; Hayashi, H.; Murai, H.; I'Haya, Y. J. *J. Am. Chem. Soc.* **1988**, *110*, 7479.
(20) Moroi, Y.; Braun, A. M.; Grätzel, M. *J. Am. Chem. Soc.* **1979**, *191*, 567.
(21) Barra, M.; Calabrese, G. S.; Allen, M. T.; Redmond, R. W.; Sinta, R.; Lamola, A. A.; Small, R. D., Jr.; Scaiano, J. C. *Chem. Mater.* **1991**, *3*, 610.
(22) Shida, T. *Electronic absorption spectra of radical ions*; Elsevier: Amsterdam, The Netherlands, 1988.
(23) Petrov, N. Kh.; Borisenko, V. N.; Starostin, A. V.; Alfimov, M. V. *J. Chem. Phys.* **1992**, *96*, 2901.
(24) Fujita, H.; Yamauchi, J. *J. Heterocycl. Chem.* **1980**, *17*, 1053.
(25) Rieger, P. H.; Bernel, I.; Reimuth, W. H.; Frankel, G. K. *J. Am. Chem. Soc.* **1963**, *85*, 683.
(26) Yim, M. B.; Wood, D. E. *J. Am. Chem. Soc.* **1976**, *98*, 2053.
(27) Murai, H.; Kuwata, K. *Chem. Phys. Lett.* **1989**, *164*, 567.
(28) Batchelor, S. N.; Heikkilä, H.; Kay, C. W. M.; McLauchlan, K. A.; Shkrob, I. A. *Chem. Phys.* **1992**, *162*, 29.
(29) Kowert, B. A.; Marcoux, L.; Bard, A. J. *J. Am. Chem. Soc.* **1972**, *94*, 5538.
(30) Weller, A.; Nolting, K.; Steark, H. *Chem. Phys. Lett.* **1983**, *96*, 24.
(31) Turro, N. J.; Grätzel, M.; Braun A. M. *Angew. Chem., Int. Ed. Engl.* **1980**, *19*, 675.
(32) Basu, S.; Kundhu, L.; Chowdhury, M. *Chem. Phys. Lett.* **1987**, *141*, 115.
(33) Batchelor, S. N.; Kay, C. W. M.; McLauchlan, K. A.; Shkrob, I. A. *J. Phys. Chem.* **1993**, *97*, 13250.
(34) Steiner, U. E.; Wu, J. Q. *Chem. Phys.* **1992**, *162*, 53.
(35) Yonemura, H.; Nakamura, H.; Matsuo, T. *Chem. Phys. Lett.* **1989**, *155*, 157.
(36) Batchelor, S. N.; Kay, C. W. M.; McLauchlan, K. A.; Shkrob, I. A. *Mol. Phys.* **1992**, *75*, 501.
(37) Sakuragi, H.; Nakagaki, R.; Oguchi, T.; Arai, T.; Tokumaru, K.; Nagakura, S. *Chem. Phys. Lett.* **1987**, *135*, 325.
(38) Nakamura, Y.; Igarashi, M.; Sakaguchi, Y.; Hayashi, H. *Chem. Phys. Lett.* **1994**, *217*, 387.
(39) Wakasa, M.; Sakaguchi, Y.; Hayashi, H. *Mol. Phys.* **1994**, *83*, 613
(40) Noyes, R. M. *J. Am. Chem. Soc.* **1956**, *78*, 5486.
(41) Kaptain, R. *J. Am. Chem. Soc.* **1971**, *94*, 6251.
(42) Aminov, K. L.; Pedersen, J. B. *Chem. Phys.* **1995**, *193*, 297.
(43) Wakasa, M.; Nakamura, Y.; Sakaguchi, Y.; Hayashi, H. *Chem. Phys. Lett.* **1993**, *215*, 631.
(44) Marcus, R. A. *J. Phys. Chem.* **1956**, *24*, 979.
(45) Rehm, D.; Weller, A. *Isr. J. Chem.* **1970**, *8*, 259.
(46) Kawanishi, Y.; Kitamura, N.; Tazuke, S. *J. Phys. Chem.* **1986**, *90*, 2469.
(47) Wakasa, M.; Sakaguchi, Y.; Nakamura, J.; Hayashi, H. *J. Phys. Chem.* **1992**, *96*, 9651.
(48) Petit, M. A.; Thami, T.; Lelièvre, D. *New J. Chem.* **1991**, *15*, 71.